Abdominal Radiology (2019) 44:2822–2834
https://doi.org/10.1007/s00261-019-02060-w

PANCREAS

CT and MR imaging features of pancreatic adenosquamous carcinoma and their correlation with prognosis

Rui Zhao[1] · Zhenyu Jia[2] · Xiao Chen[1] · Shuai Ren[1] · Wenjing Cui[1] · Deng-ling Zhao[3] · Shaojuan Wang[1] · Jianhua Wang[1] · Tao Li[4] · Yong Zhu[1] · Xiaowen Tang[1] · Zhongqiu Wang[1]

Published online: 11 June 2019

Abstract

Purpose To retrospectively investigate the computed tomography (CT) and magnetic resonance (MR) imaging features of pancreatic adenosquamous carcinoma (PASC) and the association between imaging findings and prognosis.

Materials and methods CT, MR images of 26 patients with PASC were analyzed. Clinical symptoms, tumor markers, and patients' survival were recorded. Tumor attenuation, enhancement pattern and degree, vessel involvement, adjacent tissue invasion and metastasis were evaluated. The association between imaging features and overall survival (OS) were also assessed using Cox proportional hazards ratio model.

Results Fourteen masses were found in the head of the pancreas and 12 in the body/tail. The mean tumor size was 4.47 ± 1.76 cm. PASC usually showed ill-defined (96.2%), lobulated (76.9%) and predominantly solid mass (92.3%). Ring enhancement in the peripheral area of the tumor was commonly seen (76.9%). Vessel invasion was seen in 17 cases (65.4%), encasement of adjacent arteries in 7 cases (26.9%), upstream main pancreatic duct (MPD) dilatation in 16 cases (61.5%) and double duct sign in 9 cases (34.6%). Multivariate Cox proportional hazards model demonstrated that patients with vessel invasion may predict a poor prognosis ($p = 0.037$).

Conclusion PASC tends to be an ill-defined solid mass with peripheral ring enhancement, and relatively poor enhancement in the central area. PASC may also show vessel invasion, vessel encasement and upstream MPD dilatation. Vessel invasion may indicate a poor prognosis.

Keywords Pancreatic neoplasm · Carcinoma, adenosquamous · Multidetector computed tomography · Magnetic resonance imaging

Introduction

Pancreatic adenosquamous carcinoma (PASC), a rare subtype of pancreatic carcinoma, accounting for only 1–4% of exocrine pancreatic malignancies [1], demonstrates both malignant squamous and glandular differentiation. PASC has an aggressive clinical course and a poor prognosis, with a median overall survival (OS) of 4.0–10.9 months [1–4]. Patients with PASC can benefit from surgical resection [1, 3, 5] and adjuvant chemoradiotherapy (CRT) [2, 6], and squamous cancer tissue is sensitive to radiation therapy. It has reported that a patient with PASC survived for 40 months after extended radical surgery, intraoperative radiation therapy, and locoregional chemotherapy [7].

However, lacking specific symptoms, tumor markers, together with knowing less about the imaging features of PASC makes it difficult to be differentiated from pancreatic

Electronic supplementary material The online version of this article (https://doi.org/10.1007/s00261-019-02060-w) contains supplementary material, which is available to authorized users.

✉ Zhongqiu Wang
zhq2001us@163.com

1 Department of Radiology, The Affiliated Hospital of Nanjing University of Chinese Medicine, 155 Hanzhong Road, Nanjing 210029, China

2 Department of Interventional Radiology, The First Affiliated Hospital with Nanjing Medical University, 300 Guangzhou Road, Nanjing 210029, China

3 Department of Radiology, Zhongda Hospital, School of Medicine, Southeast University, 87 Dingjiaqiao, Nanjing 210009, China

4 Department of Pathology, The First Affiliated Hospital with Nanjing Medical University, 300 Guangzhou Road, Nanjing 210029, China

ductal adenocarcinoma (PDAC). Recent studies (8–23 cases) and case reports have demonstrated various imaging features of PASC, such as ring and progressive enhancement, extensive necrosis or lack of pancreatic atrophy [8–12]. The CT and MR imaging features of PASC need further clarification in larger series. In addition, the association between imaging features and prognosis has not yet been elucidated. In this study, we investigated the CT and MR imaging features in 26 patients with PASC, and evaluated the features that are prognosis-related.

Materials and methods

Patients

From January 2010 to June 2018, a total of 29 patients with pathologically proven PASC from three institutions were collected. One patient with recurrent PASC, and another two with a history of carcinoma in other sites were excluded from this study. Thus, 26 patients were included. Twenty-five patients were diagnosed on specimens obtained by surgical resection and one patient was diagnosed by biopsy. Patients' demographics, presenting symptoms, tumor markers such as carbohydrate antigen (CA 19-9, CA 125), carcinoembryonic antigen (CEA) and outcome were recorded. This multicenter retrospective study was approved by the institutional review board with waiver of informed consent.

Imaging examinations

Dynamic CT and MR imaging

Twenty-six patients were examined by CT or MRI (only by CT, $n=18$; only by MRI, $n=1$; by CT & MRI, $n=7$). Both unenhanced and contrast-enhanced CT images were obtained in 25 patients. The following MDCT scanners were used: SOMATOM Definition, Siemens Healthcare, Germany ($n=9$); Philips Brilliance 64, Philips Healthcare, Best, the Netherlands ($n=7$); Optima 670, GE Healthcare, USA ($n=5$); GE Light Speed 64VCT, GE Healthcare, USA ($n=4$). The scanning parameters were as follows: detector collimation of 64×0.5–0.625 mm, gantry rotation time of 0.4–0.5 s, tube voltage of 120 kVp, tube current of 160–250 mAs, slice thickness of 3–5 mm, slice interval of 3.0 mm, and a reconstruction interval of 1.25 mm. Contrast-enhanced CT was performed after the intravenous injection of 80–100 mL non-ionic contrast material (iopromide, 300 mg I/mL, Schering, Germany; iohexol, Omnipaque, 350 mg I/mL, GE Healthcare) at a rate of 3–4 mL/s through antecubital vein. The enhanced CT was obtained at mean time of 35 s for the arterial phase (AP), 60 s for the portal venous phase (PVP), and 120 s for the delayed phase (DP) after contrast injection.

MR scanning was performed using 1.5 T or 3.0 T scanner (Siemens, Magnetom Aera ($n=5$); Siemens, Magnetom Verio ($n=3$)) with 18-channel or 6-channel phased-array receiver coil. Baseline MR sequences included breath-hold transverse T2-weighted turbo spin echo (TSE) sequence with fat saturation, breath-hold T1-weighted in- and out-of-phase three-dimensional gradient-echo sequence, breath-hold T1-weighted fat-suppressed volumetric interpolated breath-hold examination (VIBE), diffusion-weighted imaging (DWI) with b values of 0, 400 and 800 s/mm^2, breath-hold coronal T2-weighted images with half-fourier acquisition single-shot turbo spin echo (HASTE), and MR cholangio pancreatography. Enhanced MRI scan was performed in 5 patients. Dynamic MR images were obtained by using fat-suppressed T1-weighted three-dimensional VIBE before and after the injection of gadopentetate dimeglumine (Magnevist, Bayer HealthCare, Berlin, Germany) (dose, 0.1 mmol/kg; rate, 2–3 mL/s) with a power injector. AP, PVP and DP images were obtained at 25–35 s, 60–70 s, 120–130 s after contrast injection. Detailed MR imaging parameters are summarized in Table 1.

Table 1 MR imaging acquisition parameters

Parameters	T1-weighted imaging		T2-weighted imaging		Diffusion-weighted imaging		Dynamic imaging	
	3.0 T	1.5 T	3.0 T	1.5 T	3.0 T	1.5 T	3.0 T	1.5 T
TR (ms)	3.9	4.9	2000	2200	8300	4800	3.9	4.9
TE (ms)	1.4	2.3	70	76	76	56	1.4	2.3
FA (degree)	9.0	10	140	160	–	–	9.0	10
Section thickness (mm)	3	3	5	5	5	6	3	3
FOV (mm)	320–380	320–400	300–380	300–380	300–340	300–340	320–380	320-400
Matrix	182×320	176×288	320×285	168×320	63×130	55×140	182×320	176×288

TR repetition of time, *TE* echo time, *FA* flip angle, *FOV* field of view

Imaging analysis

All the images of CT and MRI were reviewed by two radiologists with more than 10 years' experience in abdominal radiology. They independently assessed these patients in a random order. Any disagreements were resolved by a third abdominal radiologist with more than 20 years' experience. The imaging features were evaluated with the following parameters: (a) tumor location; (b) tumor maximal diameter; (c) tumor shape; (d) tumor margin; (e) tumor attenuation; (f) signal intensity on T1 and T2-weighted MR image; (g) enhancement pattern and degree; (h) vessel invasion and encasement; (i) MPD and common bile duct (CBD) dilatation; (j) peripancreatic structure invasion; (k) positive lymph node and metastasis.

We categorized tumor attenuation into predominantly cystic (necrotic or cystic area making up more than 50%), or predominantly solid (necrotic or cystic area making up less than 50%). We measured the CT attenuation in both the peripheral and the central areas of the lesion in all phases on the slice which the lesion demonstrated the maximal diameter. Four region-of-interest (ROIs) in each area were drawn (Fig. 1). Then, the values of 4 ROIs (mean 45 mm^2, range 25–75 mm^2) were averaged as the final CT attenuation. The attenuation of normal pancreas was measured in the same method. Enhancement degree was classified as mild (less than 30 HU), moderate (30–50 HU) or intense enhancement (more than 50 HU), according to the difference in tumor attenuation between contrast and non-contrast CT.

Vessel invasion was defined according to NCCN guideline (v 2.2017) [13]. Tumor-vascular contact with hazy fat plane, vascular contour irregularity or focal vessel narrowing, vascular occlusion or tumor thrombosis, or dilated peripancreatic collateral vessels were considered to be vascular invasion. Vessel encasement was defined as tumor contact with more than 180° of the vessel circumference [14]. Pancreatic segmental portal hypertension is known as sinistral portal hypertension, caused by thrombosis or obstruction of the portal venous system (mainly splenic vein). The involvement of these vessels often results in the dilatation of collateral vessels. Upstream MPD and CBD were considered as dilated if it was greater than 3 mm and 8 mm in diameter, respectively.

Follow-up

We did the follow-up until June 2018. The survival of 16 patients were available. The other ten patients dropped out of follow-up.

Pathology analysis

The histologic specimens and diagnoses were reviewed by three pathologists at three hospitals. PASC was diagnosed when malignant squamous cells (more than 30%) and adenocarcinoma cells [1, 15] were observed by hematoxylin–eosin (H-E) staining. The peripheral and central area of tumor, and the invasion of adjacent structure were reviewed. We also assessed the tumor-vascular invasion, mainly in the major vessels. Most of the tumor's histologic features were further confirmed by immunohistochemistry (CK5/6, P40, P63, CK7, CK19) [6].

Statistical analysis

Statistical analysis was performed with SPSS 24.0 software. The mean maximal diameters of the tumor in different location of pancreas were compared with student's *t* test.

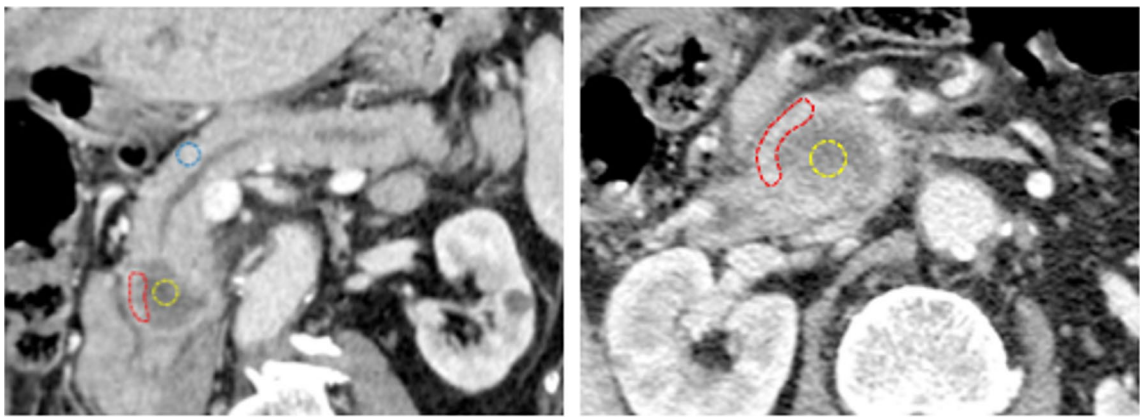

Fig. 1 The diagram of measuring CT attenuation of the tumor and normal pancreas in each phase. We measured the CT attenuation in both the peripheral (red line area) and the central areas (yellow circle area) of the lesion. Four region-of-interest (ROIs) in each area were drawn. Then, the values of 4 ROIs (mean 45 mm^2, range 25–75 mm^2) were averaged as the final value. The attenuation of normal pancreas (blue circle area) was measured in the same method

Survival curve was obtained using Kaplan–Meier method. Multivariate survival analysis was performed using Cox proportional hazards ratios model. $p < 0.05$ was considered statistically significant.

Results

Clinical characteristics

Patients' clinical characteristics are shown in Table 2. The mean age of the patients at diagnosis was 65.2 ± 12.0 years (range 40–86 years). Primary symptoms included abdominal pain (in 81.0%), jaundice (in 33.3%) and weight loss (in 42.9%). Of the 16 patients whose tumor markers had been tested, CA 19-9 elevated in 12 patients (12/16, 83.3%, reference value < 37 U/mL), and CA 125 elevated in 5 patients (5/16, 31.2%, reference value < 35 U/mL).

CT and MR imaging findings

The CT and MR imaging findings of PASC are summarized in Table 3. Fourteen lesions (53.8%) were located in the head of the pancreas, and 12 lesions (46.2%) in the body and/or tail. The mean maximal diameter of the tumor was

Table 2 Clinical features, tumor markers, immunohistochemistry in 26 patients with adenosquamous carcinoma of the pancreas (PASC)

Variables	Number	%
Gender		
Male	15	57.7
Female	11	42.3
Age mean ± SD (year)	65.2 ± 12.0	
Symptom[a]		
Abdominal pain	17	81.0
Jaundice	7	33.3
Weight loss	9	42.9
Tumor marker[b]		
CEA	0	0
CA19-9	12	75
CA125	5	31.2
Immunohistochemistry results[c]		
CK5/6(+)	8	44.4
P40(+)	10	55.6
P63(+)	14	77.8
CK7(+)	11	61.1
CK19(+)	8	44.4

[a]The symptoms of 21 patients are available among the 26 patients

[b]16 patients have the results of these three tumor markers

[c]Among the 26 patients, 18 of them have the immunohistochemistry results

Table 3 CT and MR imaging findings of 26 patients with PASC

CT and MRI findings	Number/value	%
Tumor location		
Head	14	53.8
Body and tail	12	46.2
Tumor maximal diameter(mean)[a]	4.47 ± 1.76	
Head	3.83 ± 1.44	
Body and tail	5.21 ± 1.86	
Shape		
Round	6	23.1
Lobulated and irregular	20	76.9
Margin		
Well circumscribed	1	3.8
Ill-defined	25	96.2
Partially exophytic growth		
Yes	4	15.4
No	22	84.6
Texture		
Predominantly solid	24	92.3
Predominantly cystic	2	7.7
Signal intensity		
T1WI		
Slight hypointensity	7	87.5
Hypointensity	1	12.5
T2WI		
Heterogenous hyperintensity	7	87.5
Homogenous hyperintensity	1	12.5
Calcification[b]	1	3.8
Vessel invasion		
Yes	17	65.4
No	9	34.6
Vessel encasement		
Yes	7	26.9
No	19	73.1
MPD dilatation	16	61.5
Double duct sign	9	34.6
Pancreatic atrophy	11	42.3
Peripancreatic invasion		
Duodenum	10	38.5
Stomach	3	11.5
Spleen	3	11.5
Kidney or adrenal gland	2	7.7
Metastasis		
Liver	2	7.7
Lymph node	6	23.1

[a]The tumor diameter of pancreatic head is smaller than tumor in body and tail, they are of statistical significance ($p = 0.043$)

[b]The patient who only performed MRI is excluded when evaluating whether calcification exists or not

4.47 ± 1.76 cm (range 1.9–8.9 cm). The mean diameter of the tumor located in pancreatic body/tail was larger than that in the head (5.21 ± 1.86 cm vs. 3.83 ± 1.44 cm, $p = 0.043$). Six lesions (23.1%) were round or oval and 20 (76.9%) were lobulated or irregular. Tumors were ill-defined in 25 cases (96.2%) and well-defined in 1 case (3.8%). Tumors showed exophytic growth pattern in 4 cases.

Predominantly solid mass (Figs. 2, 3, 4, 7a–c) was found in 24 cases (92.3%), and predominantly cystic lesion (Figs. 7d–f) in 2 cases (7.7%). Calcification was found in 1 case, upstream MPD dilatation in 16 cases, CBD dilatation in 10 cases, double duct sign in 9 cases, and distal pancreatic atrophy in 11 cases.

In unenhanced CT, the masses showed isoattenuation or heterogeneous hypoattenuation. Irregular or incomplete ring enhancement was found in 20 cases (76.9%) (Figs. 3, 4). Thirteen of them showed a thick ring (> 3 mm) (Figs. 3a, b) and seven exhibited a thin ring (< 3 mm) (Figs. 3c, d). In addition, 14 rings (70%) showed moderate enhancement (Figs. 3c, d), 3 intense enhancement (Figs. 3a, b), and 3 mild enhancement (Figs. 3e, f). The central area of the tumor showed relatively poor enhancement in 24 cases (92.3%) and progressive enhancement (Table 4, Fig. 4) in 20 cases (76.9%).

The mean CT attenuation in the peripheral area of the tumor was 38.25 ± 6.17 HU in unenhanced CT, 81.8 ± 22.51 HU in AP, 102.6 ± 14.20 HU in PVP, and 101.7 ± 12.72 HU in DP. The curve of time-density showed that the mean attenuation in AP in the periphery of the tumor was similar to the normal pancreas, and that

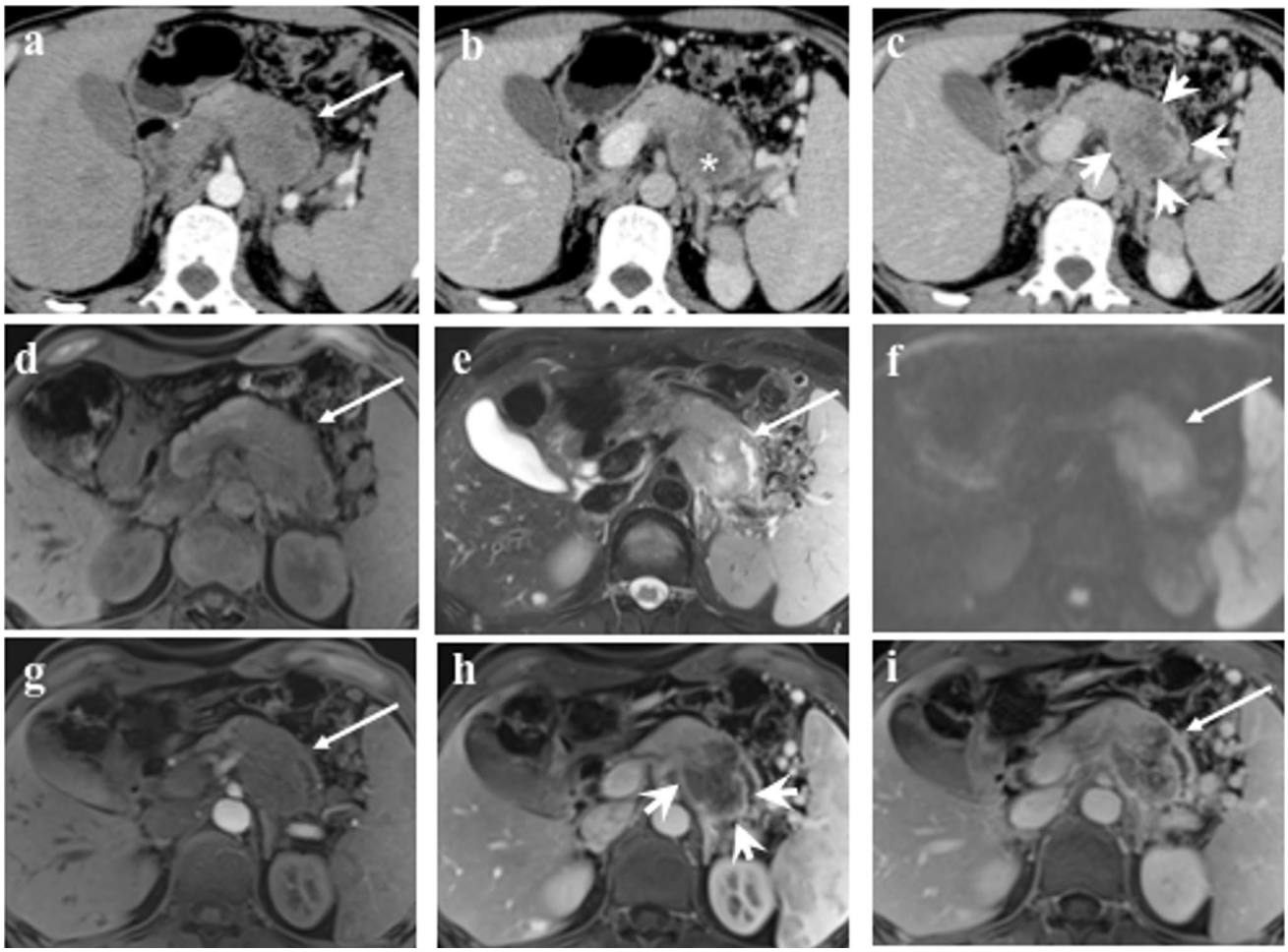

Fig. 2 CT and MR images of a 59-year-old man with PASC. **a** Axial CT arterial phase (AP) image shows an ill-defined solid mass in pancreatic body and tail. **b** and **c** Portal vein phase (PVP) and delayed phase (DP) images show thin enhanced ring (short arrow) in the peripheral area of the tumor and hypoenhancement (white star) in the central area of the mass. Besides, the dilated peripancreatic collateral vessels are seen. **d** Axial T1-weighted image shows a slight hypointense tumor with ill-defined margin. **e** and **f** Axial T2-weighted and diffusion-weighted image (DWI) ($b = 800$ s/mm^2) show a slight hyperintense tumor with distal main pancreatic duct (MPD) dilatation. **g–i** Dynamic-enhanced images show thin enhanced ring (short arrow) in the periphery of the tumor in PVP (**h**), and progressive increasing delayed enhancement in the central hypovascular area of the tumor in DP (**i**)

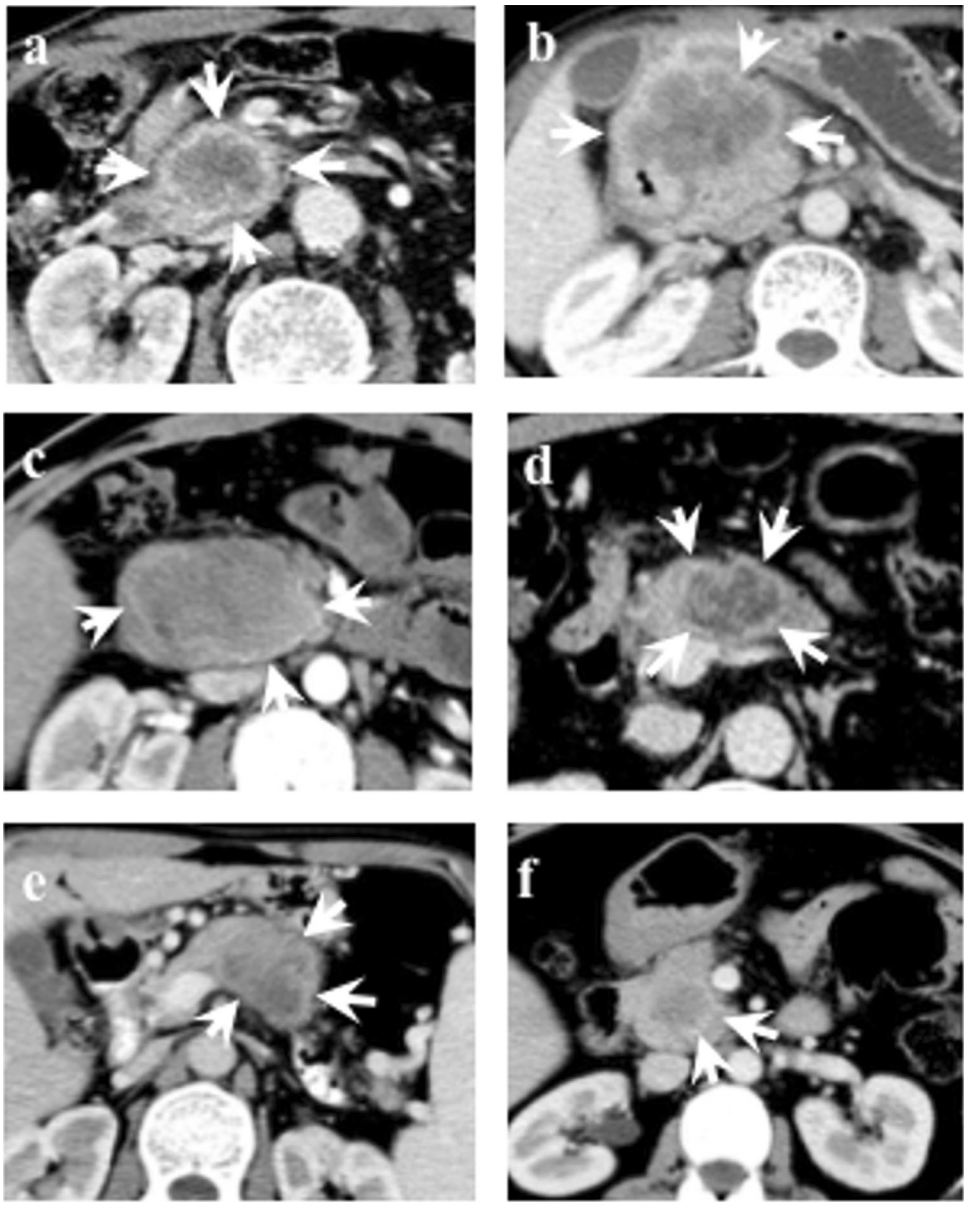

Fig. 3 Different types of ring enhancement in the peripheral area of PASC. **a** and **b** Masses in the head of the pancreas in a 76-year-old man (**a**) and a 56-year-old man (**b**) exhibit intensely enhanced thick ring (> 3 mm) (short arrow) in the peripheral area. **c** and **d** A mass in the head of the pancreas in a 40-year-old man (**c**) and a mass in the body of the pancreas in a 70-year-old man (**d**) show moderately enhanced thin ring (< 3 mm) (short arrow). **e** and **f** A mass in the body of the pancreas in a 48-year-old man (**e**) and a mass in the head of pancreas in a 47-year-old woman (**f**) show mildly enhanced ring (short arrow)

in PVP and DP was slightly higher than the normal pancreas (Fig. 5), but the mean attenuation in the central area was lower than that in the periphery area and the normal pancreas.

Adjacent vessels in 17 masses (65.4%) were invaded (Figs. 6a, b), including celiac artery, superior pancreaticoduodenal artery, splenic artery/vein, portal vein, superior mesenteric artery/vein and renal artery/vein. Vessel encasement of celiac artery or splenic artery was found in seven masses (26.9%) (Figs. 6c–f). Pancreatic segmental portal hypertension was seen in ten cases (38.5%).

Local invasion into adjacent fat tissue, duodenum, stomach, spleen, kidney or adrenal gland was noted in 10, 10, 3, 3 and 2 cases, respectively. Enlarged lymph nodes were seen in six cases (23.1%), mostly along the superior mesenteric artery and portal vein, or in retroperitoneal area. Liver metastases were found in two cases (Fig. 7f).

The solid portions of all eight lesions demonstrated hypointense signal on T1-weighted images, and slight hyperintense signal on T2-weighted images and DWI (Figs. 2d–f). In one case with predominantly cystic lesion, the cystic area of the tumor showed homogeneous hypointense signal on T1-weighted images and hyperintense signal on T2-weighted images. The solid portion of the tumor showed slight hyperintense signal on DWI, but hypointense signal on ADC images. Ring and progressive enhancement (Figs. 2h, i) or vessel invasion were also found. For the patients who had undergone both CT and MRI, most of their images showed similar features. However, the ring enhancement on MR images was clearer than on CT.

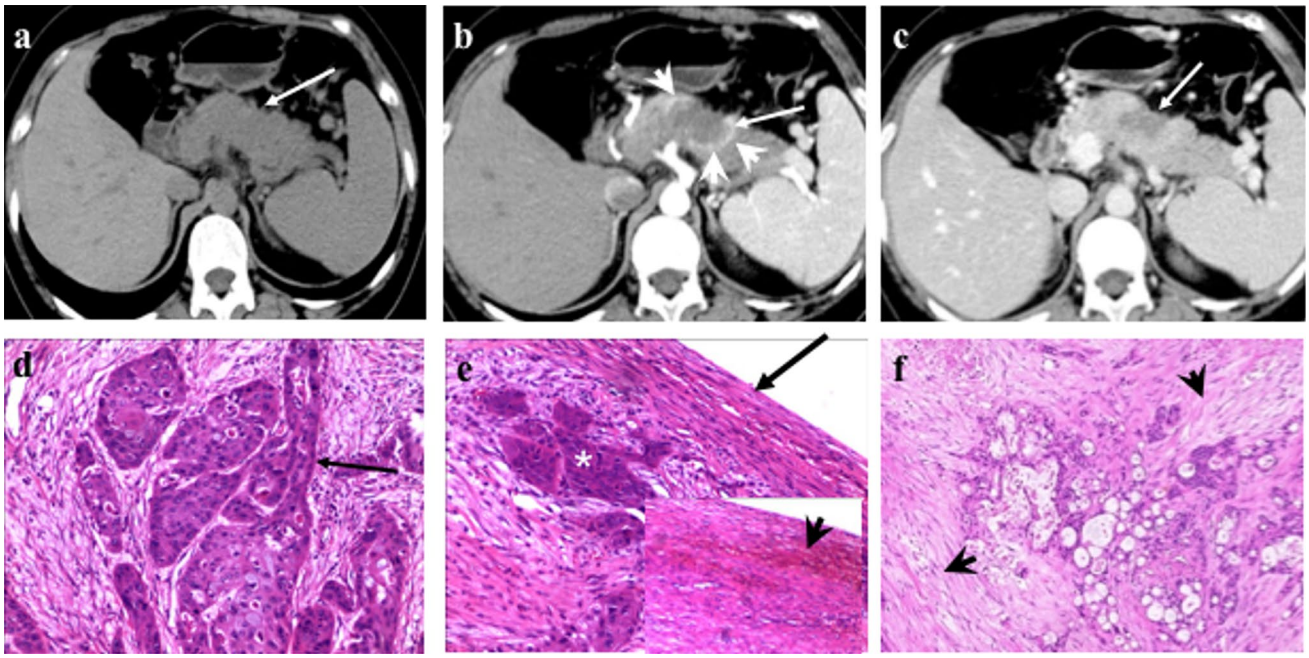

Fig. 4 PASC in the body of the pancreas in a 48-year-old woman. **a**–**c** Axial precontrast (**a**), AP (**b**) and PVP (**c**) CT images show an isodense mass (white arrow) with incomplete thick ring (short arrow) with intense enhancement, while the central area shows progressive poor enhancement (white arrow). **d** Haematoxylin–eosin (H-E) stained image shows the lesion contained nests of squamous carcinoma cells (black arrow) (original magnification, × 100). **e** The tumor is encapsulated by fibrous tissue (black arrow). Plenty of capillary vessels (short black arrow) and squamous carcinoma cells (white star) are seen in the margin of the tumor (original magnification, × 40). **f** Abundant fibrous stroma (short black arrow) is seen around the tumor cells in the central area (original magnification × 100)

Table 4 Enhancement pattern and degree of PASC after contrast injection

Enhancement pattern and degree	Number	%
Peripheral area		
Ring enhancement	20	76.9
Thick ring	13	65
Thin ring	7	35
Enhancement degree of the ring		
Mildly	3	15
Moderately	14	70
Intense	3	15
Central area		
Progressive enhancement	20	76.9
Enhancement degree		
Mildly	24	92.3

Histopathology findings

HE-stained images exhibited squamous (Fig. 4d) and adenocarcinomatous tissues intermingling with each other (the squamous tissues accounting for 30–80% of the tumor). All the tumors were moderately or poorly differentiated.

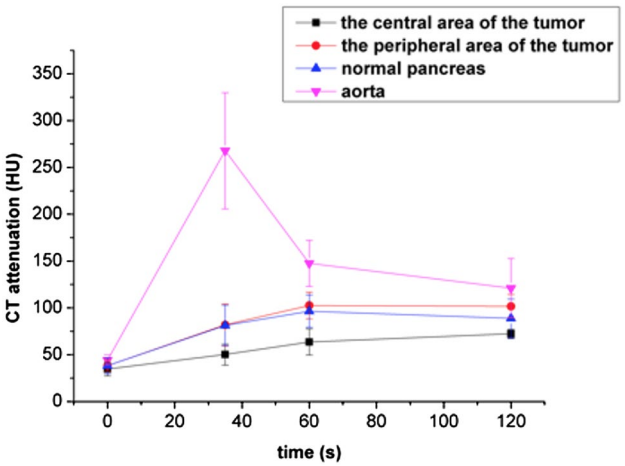

Fig. 5 Dynamic contrast-enhanced curve of PASC. The curve of time-density shows the mean attenuation in the periphery area of the lesion is similar to that in the normal pancreas in AP, and is slightly higher than that in the normal pancreas in PVP and DP, whereas the mean attenuation in the central area is lower than that in the periphery or the normal pancreas in each phase. The central area of the lesion shows progressive enhancement pattern

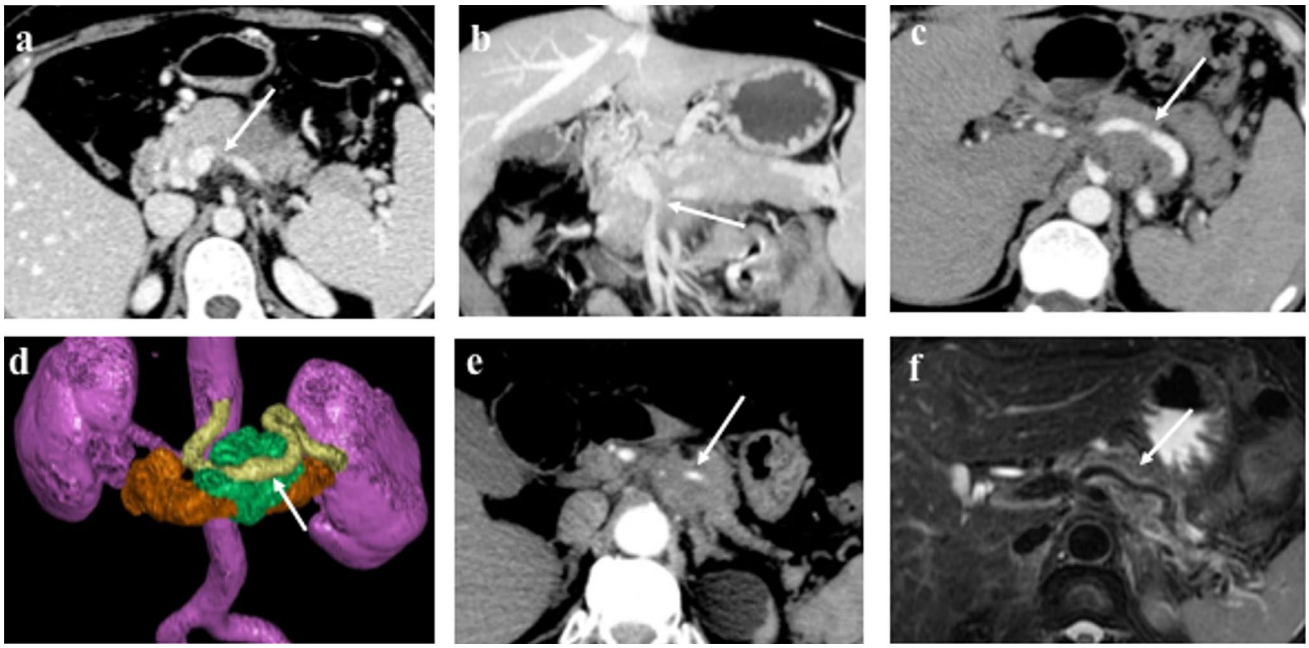

Fig. 6 Vessel invasion and vessel encasement by PASC **a** and **b** show the vessel invasion into the portal vein system (white arrow) by the mass in a 48-year-old woman. **c** and **d** show the vessel encasement of splenic artery by the mass (white arrow) in a 59-year-old man in CT axial AP image and 3D tissue segmentation image. **e** and **f** CT axial AP and T2-weighted images show the encasement of splenic artery (arrow) without luminal stenosis in a 73-year-old woman (**e**) and a 68-year-old woman (**f**)

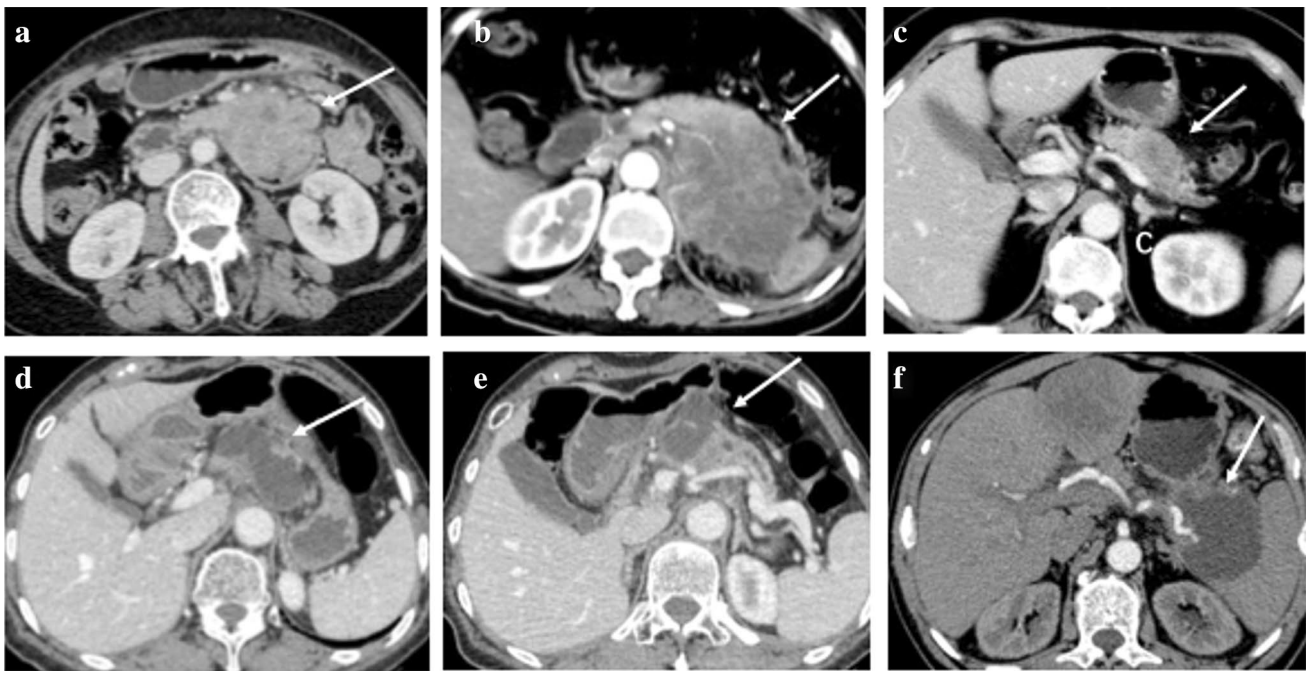

Fig. 7 Uncommon CT imaging features of pathologically proven PASC. **a** Axial PVP CT image shows a predominantly solid tumor in the uncinate process of pancreas (arrow) in a 66-year-old woman. The mass does not show ring enhancement but exhibits exophytic growth pattern. **b** Axial PVP CT image shows a large exophytic mass located in the pancreatic body and tail in a 53-year-old woman. The vessel invasion into the splenic artery (arrow) by the mass is seen. **c** Axial PVP CT image shows a predominantly solid hypovascular tumor in the body of pancreas (arrow) in a 72-year-old woman, exhibiting relatively hypovascular. **d** and **e** Axial PVP CT image shows a predominantly cystic tumor in the body of pancreas (arrow) in a 75-year-old woman. **f** Axial AP CT image shows a predominantly cystic tumor in the tail of pancreas (arrow) in a 75-year-old man. Encasement of splenic artery is seen in the tumor

The tumor was encapsulated by an incomplete thin layer of fibrous tissue (Fig. 4e). Squamous carcinoma cells and rich blood vessels (Fig. 4e) were commonly found in the margin of the tumor. Squamous carcinoma was admixed with adenocarcinoma, necrosis and fibrous stroma (Fig. 4f) in the central area of the tumor. The pathology results showed that the invasion into adjacent tissues and major vessels were well consistent with the changes in CT and MRI images. Moreover, most of the tumors were CK5/6, P40, P63, CK7 and CK19 positive.

Patients' survival

Sixteen patients were followed up for 1–25 months with mean and median follow-up 9.8 and 9 months, respectively. The mean and median OS (Fig. 8a) after surgical resection was 10.67 and 10 months, respectively. Only one patient survived more than 2 years. The cumulative survival rate was 61.4% at 6 months, 9.4% at 1 year. Five patients who received adjuvant chemotherapy after surgery had a longer mean survival of 14.2 months. Multivariate Cox proportional hazards model demonstrated that the patients with vessel invasion showed a less-favorable survival compared to those without vessel invasion (hazard ratio (HR) = 1.35, 95% CI 1.19–1.58; $p = 0.037$), after adjustment for gender, age, tumor size and tumor location (Fig. 8b).

Discussion

PASC is a rare type of pancreatic malignancy, characterized by a mixture of squamous tissues with adenocarcinoma [15]. PASC has a poorer survival compared with PDAC, and it is difficult to be differentiated from PDAC and other malignancies preoperatively. Given the rarity of PASC, only several radiologic reports of this tumor with small sample sizes have been published [8–11]. Our study differs from the previous, in that we not only analyzed the imaging features in a relatively larger series of PASC to date, but also evaluated their association with survival. PASC in our series commonly shows predominantly solid mass with a central poor enhancement area. However, extensive central necrosis was commonly seen according to previous radiological reports [8–11, 16–18]. A possible explanation may be that the predominantly solid tumor in our series had relatively rich blood supply (with CT attenuation of 81.8 ± 22.51 HU in AP for the peripheral area of the tumor), so the squamous carcinoma cells might be less likely to undergo extensive necrosis.

The present study demonstrated that most of the PASC had characteristic radiological features, which brings a possibility of precisely diagnosing and treating in clinical practice. The typical imaging feature in our series was the ring enhancement pattern in the periphery of the tumor (20/26, 76.9%). The enhanced ring demonstrated different thickness and enhancement, which may be associated with the high heterogeneity of the tumor. The curve of time-density also showed that PASC was a relatively hypervascular tumor for the peripheral area. According to Imaoka et al., ring enhancement was considered as the most useful imaging parameter to predict PASC with sensitivity of 65.2% and specificity of 89.6% [11]. Not commonly (less than 20%) seen in PDAC [19], ring enhancement may be valuable in the differential diagnosis between PDAC and PASC. In addition, our pathology results showed that many squamous carcinoma cells and vessels were frequently found in the periphery of the tumor, probably due to the reason that squamous carcinoma cells need more blood supply. This pathologic feature may explain the ring enhancement pattern.

For the central area, most of the tumors showed relatively poor and progressive enhancement, indicating that this area may contain hypovascular neoplastic cells, necrosis or fibrous stroma. These speculations are consistent with our pathology results. Previous studies inferred that central hypodense area of PASC was occupied by squamous carcinoma or large foci of squamous carcinoma, and that squamous component was more likely with the occurrence of necrosis than adenocarcinoma [20–22]. However, the present study showed that different amounts of adenocarcinoma admixed with squamous cell carcinoma were commonly found in the central area, which is not absolutely consistent with previous results. Further confirmation is needed in the future.

Another characteristic of PASC was its peritubular growth, manifested with vessel involvement and double duct sign. Previous studies indicated that the squamous component in PASC was more likely to show vascular invasion [2, 4]. In our study, the tumor invaded into adjacent vessels in more than half of the cases. However, the tumors did not demonstrate the selective vascular invasion (marked portal system invasion without arterial invasion) [16]. In addition, the encasement of the vessel usually involved celiac artery or splenic artery. The reason may be that the arterial wall, thicker than the venous wall, is not easy to be invaded. Besides, tumor thrombus was found in three patients, an incidence similar to previous findings.

In our series, double duct sign and pancreatic atrophy were commonly observed. Upstream MPD and CBD dilatation was seen in 16 and 10 patients, which is similar to previous findings [8–10]. The double duct sign benefits the differential diagnosis of pancreatic neoplasms. Solid pseudopapillary tumor (SPT), neuroendocrine tumors (NETs), and acinar cell carcinoma (ACC) usually do not involve CBD and MPD. Pancreatic tissue distal to pancreatic cancer often show atrophy. Ding et al. reported that pancreatic atrophy was not found in their study [8]. Yin et al. reported that 4

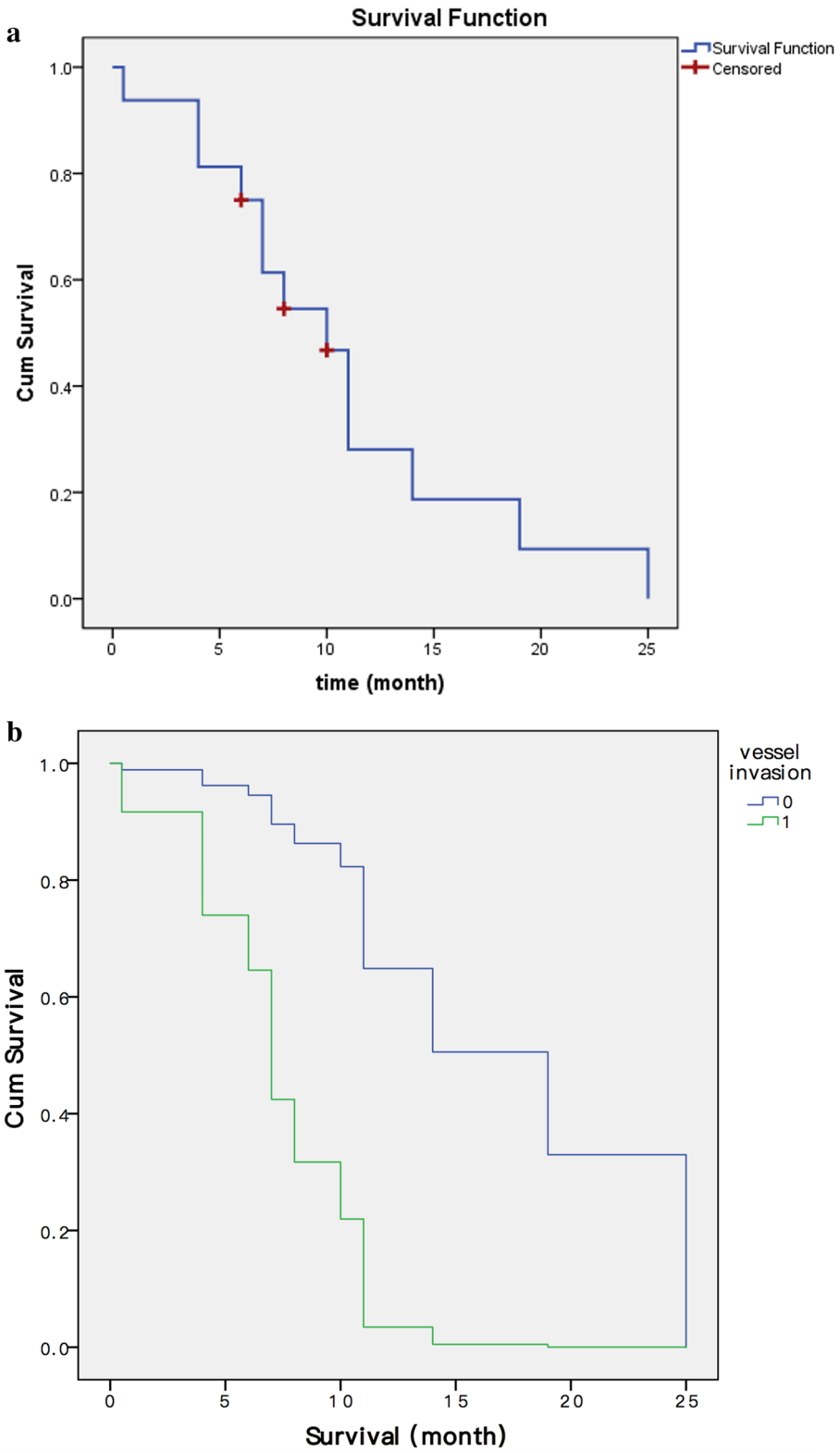

Fig. 8 Cumulative survival curve and influence of vessel invasion on survival. **a** The survival curve shows that the mean and median survival are 10.67 and 10 months, respectively. **b** Multivariate Cox proportional hazards model demonstrates that patients with vessel invasion may predict a poorer overall survival (OS) relative to patients without vessel invasion (hazard ratio (HR), 1.35; 95% CI 1.19–1.58; $p = 0.037$)

of 12 patients showed pancreatic atrophy [9]. In our study, pancreatic atrophy was seen in 11 of 26 patients.

PASC has been regarded as having an aggressive behavior and less-favorable survival [23]. Our study also showed a poor prognosis with a median OS of 10 months after resection. In the absence of distant metastasis, the degree of vascular invasion is considered as the most important factor to predict PDAC resectability and survival [24]. However, the

prognostic factors of PASC based on its imaging features have not yet been explored. In our study, only vessel invasion indicated a poor prognosis. In addition, only 6 cases (6/26, 23.1%) that exhibited lymph node enlargement on CT or MR scans in our study. A possible explanation may be that most of these masses were resectable. Thus, we did not evaluate the effect of lymph node status on survival in our study. According to Voong et al., the presence of metastatic lymph node was not predictive of survival in patients with PASC [2]. Similarly, Boyd CA et al. found that nodal status did not have any bearing on survival in patients with locoregional PASC [1].

In addition, there was no significant correlation between tumor location and patients' survival. Some reports showed that the prognosis of PASC located in the head of pancreas was better than that in the pancreatic body/tail [25]. The authors attributed this prognostic difference to the tumor size, as the distal pancreatic tumor was larger than the proximal tumor. A possible explanation may be that the tumors located in the head cause more easily detectable symptoms, such as jaundice or vomiting [6]. Similarly, in our study, the mean size of tumors located in the head/neck of the pancreas was smaller than that in the pancreatic body/tail, and the former had a better prognosis, but there was no statistical significance.

According to previous report, PASC has no specific tumor markers [25]. CA 19-9, CA125 and CEA are tumor markers to predict pancreatic adenocarcinoma, and may elevate in squamous carcinoma [5]. In some studies, both levels of CA 19-9 and CEA were elevated [5, 9], but the level of CEA was normal in other reports [7, 25]. In our study, CA 19-9 was elevated in 12 of 16 patients whose tumor marker results were available, but CEA remained normal in all the 16 patients. The difference may arise from patient selection bias.

Predominantly solid PASC should be differentiated from PDAC. PASC showed relative hyperenhancement in the peripheral area and hypoenhancement in the central area, but ring enhancement or necrosis were less commonly found in PDAC. Besides, PASC should also be differentiated from NETs, SPT, and ACC, which presenting round and solid masses with necrosis [26–30]. However, NET, typically a hypervascular neoplasm, may show a higher enhancement than pancreatic parenchyma. SPT usually occurs in young and middle-aged women, typically well-defined and well-encapsulated, and may show necrosis, hemorrhage and calcification [28, 29]. ACC typically presents as a well-defined, exophytic mass [30]. PASC with predominantly cystic tumor should be differentiated from serous cystic neoplasm (SCN), mucinous cystic neoplasm (MCN) and pseudocyst. SCN mostly occurs in women and typically presents as a multilocular cystic neoplasm with lobular shape and central stellate scar. Calcification occurs in up to 30% of cases [31]. MCN mostly affects women aged between 42 and 60 years and typically presents as a unilocular or multilocular cyst with smooth outer contour [32]. Pancreatic pseudocyst, a common non-neoplastic cystic lesion occurring after pancreatitis or trauma, can be easily differentiated from PASC with the documented history [33].

This study has several limitations. First, the number of patients with PASC was comparatively small. Second, as a retrospective study, there might have been a potential selection bias. Third, there were mild differences in scanning parameters and injection rate of contrast agent, since the patients were enrolled from three institutions. In addition, only eight patients underwent MR examinations, so the MR features of PASC need further investigation.

In conclusion, our study indicated that PASC was usually an ill-defined, predominantly solid tumor. It mainly demonstrated ring enhancement in the peripheral area and relatively poor, progressive enhancement in the central area. Vessel invasion, vessel encasement of adjacent vessels and MPD dilatation were common features. Vessel invasion may predict the poor prognosis of PASC patients.

Acknowledgements Thanks for all the authors' contributions to patient's data collection, imaging analysis, statistical analysis, and valuable suggestions.

Funding This work was supported by the National Natural Science Foundation of China (81771899) and the Key Program of Research and Development of Jiangsu Province (BE2017772).

Compliance with ethical standards

Conflict of interest The authors of this manuscript declare that they have no conflict of interest.

Informed consent Written informed consent was waived by the Institutional Review Board.

References

1. Boyd CA, Benarroch-Gampel J, Sheffield KM, Cooksley CD, Riall TS (2012) 415 patients with adenosquamous carcinoma of the pancreas: a population-based analysis of prognosis and survival. J Surg Res 174:12-19. http://dx.doi.org/10.1016/j.jss.2011.06.015
2. Voong KR, Davison J, Pawlik TM, Uy MO, Hsu CC, Winter J, Hruban RH, Laheru D, Rudra S, Swartz MJ, Nathan H, Edil BH, Schulick R, Cameron JL, Wolfgang CL, Herman JM (2010) Resected pancreatic adenosquamous carcinoma: clinicopathologic review and evaluation of adjuvant chemotherapy and radiation in 38 patients. Hum Pathol 41:113-122. http://dx.doi.org/10.1016/j.humpath.2009.07.012
3. Katz MH, Taylor TH, Al-Refaie WB, Hanna MH, Imagawa DK, Anton-Culver H, Zell JA (2011) Adenosquamous versus adenocarcinoma of the pancreas: a population-based outcomes analysis. J Gastrointest Surg 15:165-174. http://dx.doi.org/10.1007/s11605-010-1378-5

4. Komatsu H, Egawa S, Motoi F, Morikawa T, Sakata N, Naitoh T, Katayose Y, Ishida K, Unno M (2015) Clinicopathological features and surgical outcomes of adenosquamous carcinoma of the pancreas: a retrospective analysis of patients with resectable stage tumors. Surg Today 45:297-304. http://dx.doi.org/10.1007/s00595-014-0934-0
5. Kardon DE, Thompson LDR, Przygodzki RM, Heffess CS (2001) Adenosquamous carcinoma of the pancreas: a clinicopathologic series of 25 cases. Mod Pathol 14:443-451. http://dx.doi.org/10.1038/modpathol.3880332
6. Trikudanathan G, Dasanu CA (2010) Adenosquamous carcinoma of the pancreas: a distinct clinicopathologic entity. South Med J 103:903-908. http://dx.doi.org/10.1097/SMJ.0b013e3181ebadbd
7. Yamaue H, Tanimura H, Onishi H, Tani M, Kinoshita H, Kawai M, Yokoyama S, Uchiyama K (2001) Adenosquamous carcinoma of the pancreas: successful treatment with extended radical surgery, intraoperative radiation therapy, and locoregional chemotherapy. Int J Pancreatol 29:53-58. http://dx.doi.org/10.1385/IJGC:29:1:53
8. Ding Y, Zhou J, Sun H, He D, Zeng M, Rao S (2013) Contrast-enhanced multiphasic CT and MRI findings of adenosquamous carcinoma of the pancreas. Clin Imaging 37:1054-1060. http://dx.doi.org/10.1016/j.clinimag.2013.08.002
9. Yin Q, Wang C, Wu Z, Wang M, Cheng K, Zhao X, Yuan F, Tang Y, Miao F (2013) Adenosquamous carcinoma of the pancreas: multidetector-row computed tomographic manifestations and tumor characteristics, J. Comput. Assist Tomogr 37:125-133. http://dx.doi.org/10.1097/RCT.0b013e31827bc452
10. Toshima F, Inoue D, Yoshida K, Yoneda N, Minami T, Kobayashi S, Ikdeda H, Matsui O, Gabata T (2016) Adenosquamous carcinoma of pancreas: CT and MR imaging features in eight patients, with pathologic correlations and comparison with adenocarcinoma of pancreas. Abdom Radio 41:508-520. http://dx.doi.org/10.1007/s00261-015-0616-4
11. Imaoka H, Shimizu Y, Mizuno N, Hara K, Hijioka S, Tajika M, Tanaka T, Ishihara M, Ogura T, Obayashi T, Shinagawa A, Sakaguchi M, Yamaura H, Kato M, Niwa Y, Yamao K (2014) Ring-enhancement pattern on contrast-enhanced CT predicts adenosquamous carcinoma of the pancreas: a matched case-control study. Pancreatology 14:221-226. http://dx.doi.org/10.1016/j.pan.2014.02.005
12. Jiang L, Nie H, Zhu L, Xiu y, Shi HC (2017) Adenosquamous Carcinoma of the Pancreas Demonstrated on 18F-FDG PET/CT Imaging. Clin Nucl Med 42:206-208. http://dx.doi.org/10.1097/RLU.0000000000001535
13. Tempero MA, Malafa MP, Al-Hawary M, Asbun H, Bain A, & Behrman SW et al (2017) Pancreatic adenocarcinoma, version 2.2017, NCCN clinical practice guidelines in oncology. Journal of the National Comprehensive Cancer Network Jnccn 15:1028-1061. http://dx.doi.org/10.6004/jnccn.2017.0131
14. Zaky AM, Wolfgang CL, Weiss MJ, Javed AA, Fishman EK, Zaheer A (2016) Tumor-vessel relationships in pancreatic ductal adenocarcinoma at multidetector CT: different classification systems and their influence on treatment planning. Radiographics 37:93-112. http://pubs.rsna.org/doi/10.1148/rg.2017160054
15. Madura JA, Jarman BT, Doherty MG, Yum MN, Howard TJ (1999) Adenosquamous carcinoma of the pancreas. Arch Surg 134:599-603
16. Komatsuda T, Ishida H, Konno K, Sato M, Watanabe S, Furuya T, Ishida J (2000) Adenosquamous carcinoma of the pancreas: report of two cases. Abdom Imaging 25:420-423. http://dx.doi.org/10.1007/s002610000059
17. Na YJ, Shim KN, Cho MS, Sung SH, Jung SA, Yoo K, Chung KW (2011) Primary adenosquamous cell carcinoma of the pancreas: a case report with a review of the Korean literature. Korean J of Intern Med 26:348-351. http://dx.doi.org/10.3904/kjim.2011.26.3.348
18. Nabae T, Yamaguchi K, Takahata S, Utsunomiya N, Matsunaga H, Sumiyoshi K, Chijiiwa K, Tanaka M (1998) Adenosquamous carcinoma of the pancreas: report of two cases. Am J Gastroenterol 93:1167-1170. http://dx.doi.org/10.1111/j.1572-0241.1998.00299.x
19. Lee S, Kim SH, Park HK, Jang KT, Hwang JA, Kim S (2018) Pancreatic ductal adenocarcinoma: rim enhancement at MR Imaging predicts prognosis after curative resection. Radiology 288:456-466. http://pubs.rsna.org/doi/10.1148/radiol.2018172331
20. Yu JQ, Yang ZG, Austin JH, Guo YK, Zhang SF (2005) Adenosquamous carcinoma of the lung: CT-pathological correlation. Clin Radiol 60:364-369. http://dx.doi.org/10.1016/j.crad.2004.08.014
21. Yokota H, Matoba M, Tonami H, Hasegawa T, Saito H, Kurose N (2007) Imaging findings in primary adenosquamous carcinoma of the liver: a case report. Clin Imaging 31:279-282. http://dx.doi.org/10.1016/j.clinimag.2007.01.007
22. Nam KH, Kim JY (2016) Primary adenosquamous carcinoma of the liver: a case report. Clin Mol Hepatol 22:503-508. http://dx.doi.org/10.3350/cmh.2016.0077
23. Imaoka H, Shimizu Y, Mizuno N, Hara K, Hijioka S, Tajika M, Kondo S, Tanaka T, Ogura T, Obayashi T, Hasegawa T, Niwa Y, Yamao K (2014) Clinical characteristics of adenosquamous carcinoma of the pancreas: a matched case-control study. Pancreas 43:287-290. http://dx.doi.org/10.1097/MPA.0000000000000089
24. Tran Cao HS, Balachandran A, Wang H, Nogueras-González GM, Bailey CE, Lee JE, Pisters PW, Evans DB, Varadhachary G, Crane CH, Aloia TA, Vauthey JN, Fleming JB, Katz MH (2014) Radiographic tumor vein interface as a predictor of intraoperative, pathologic, and oncologic outcomes in resectable and borderline resectable pancreatic cancer. J Gastrointest Surg 18:269-278. http://dx.doi.org/10.1007/s11605-013-2374-3
25. Okabayashi T, Hanazaki K (2008) Surgical outcome of adenosquamous carcinoma of the pancreas. World J of Gastroenterol 14:6765-6770. https://dx.doi.org/10.3748/wjg.14.6765
26. Raman SP, Hruban RH, Cameron JL, Wolfgang CL, Kawamoto S, Fishman EK (2013) Acinar cell carcinoma of the pancreas: computed tomography features--a study of 15 patients. Abdom Imaging 38:137-143. http://dx.doi.org/10.1007/s00261-012-9868-4
27. Sahani DV, Bonaffini PA, Carlos FDC, Blake MA (2013) Gastroenteropancreatic neuroendocrine tumors: role of imaging in diagnosis and management. Radiology 266:38-61. http://pubs.rsna.org/doi/10.1148/radiol.12112512
28. Ganeshan DM, Paulson E, Tamm EP, Taggart MW, Balachandran A, Bhosale P (2013) Solid pseudo-papillary tumors of the pancreas: current update. Abdom Imaging 38:1373-1382. http://dx.doi.org/10.1007/s00261-013-0015-7
29. Yao X, Ji Y, Zeng M, Rao S, Yang B (2010) Solid pseudopapillary tumor of the pancreas: cross-sectional imaging and pathologic correlation. Pancreas 39:486-491. http://dx.doi.org/10.1097/MPA.0b013e3181bd6839
30. Tatli S, Mortele KJ, Levy AD, Glickman JN, Ros PR, Banks PA, Silverman SG (2005) CT and MRI features of pure acinar cell carcinoma of the pancreas in adults. AJR Am J Roentgenol 184:511-519. http://www.ajronline.org/doi/full/10.2214/ajr.184.2.01840511
31. Dietrich CF, Dong Y, Jenssen C, Ciaravino V, Hocke M, Wang WP, Burmester E, Moeller K, Atkinson NS, Capelli P (2017) Serous pancreatic neoplasia, data and review. World J of Gastroenterol 23:5567-5578. http://doi.org/10.3748/wjg.v23.i30.5567
32. Buerke B, Domagk D, Heindel W, Wessling J (2012) Diagnostic and radiological management of cystic pancreatic lesions: important features for radiologists. Clin Radiol 67:727-737. http://doi.org/10.1016/j.crad.2012.02.008

33. Barral M, Soyer P, Dohan A, Laurent V, Hoeffel C, Fishman EK, Boudiaf M (2014) Magnetic resonance imaging of cystic pancreatic lesions in adults: an update in current diagnostic features and management. Abdominal Imaging 39:48-65. http://doi.org/10.1007/s00261-013-0048-y